Molecular Modeling of Micelle Formation and Solubilization in Block Copolymer Micelles. 1. A Self-Consistent Mean-Field Lattice Theory

Patricia N. Hurter,† Jan M. H. M. Scheutjens,‡,§ and T. Alan Hatton*,†

Department of Chemical Engineering, Massachusetts Institute of Technology, Cambridge, Massachusetts 02139, and Department of Physical and Colloid Chemistry, Wageningen Agricultural University, Wageningen, The Netherlands

Received August 19, 1992; Revised Manuscript Received July 19, 1993®

ABSTRACT: A self-consistent mean-field lattice theory used to model the solubilization of polycyclic aromatic hydrocarbons in poly(ethylene oxide)–poly(propylene oxide) block copolymer micelles is able to reproduce the experimental finding that the micelle–water partition coefficient of naphthalene increases with an increase in the poly(propylene oxide) content of the polymer and with polymer molecular weight. With the polycyclic aromatic hydrocarbons treated as flexible benzene chains, the model indicated a strong correlation between the micelle–water partition coefficient and the octanol–water partition coefficient of the solute, which was also observed experimentally. Linear, triblock copolymers and starlike, branched copolymers were studied. It was found that the linear polymers formed larger micelles with a more hydrophobic core environment, resulting in higher micelle–water partition coefficients.

Introduction

Micelles formed by amphiphilic block copolymers are capable of solubilizing significant quantities of hydrophobic solutes,[1-7] which makes them attractive for a variety of practical applications, including drug delivery and separation processes. In a recent study exploring the potential for using poly(ethylene oxide)–poly(propylene oxide) (PEO–PPO) block copolymer micelles in the treatment of water contaminated with polycyclic aromatic hydrocarbons (PAHs), it was shown that solubilization efficiency depended strongly on the structure, composition, and molecular weight of the polymer used.[8] Some speculation was made as to the reasons for this behavior, but verification of these arguments, which requires either structural characterization or detailed theoretical analysis of the association and solubilization behavior of these polymer systems, is still lacking. In an attempt to address this issue, in this paper we use a self-consistent mean-field theory to study the effects of polymer structure, composition, and molecular weight on the formation of micelles by linear and branched (or starlike) amphiphilic block copolymers and on the solubilization of PAHs.

Theories of micelle formation in solutions of block copolymers have been advanced by a number of researchers over the past decade or so. Leibler et al.,[9] Noolandi and Hong,[10] Munch and Gast,[11] and Nagarajan and Ganesh[12] computed the free energy of micelle formation assuming uniform copolymer concentrations in the core and corona regions, respectively, as shown in Figure 1a. Scaling theories for polymeric micelles with an insoluble core and an extended coronta (Figure 1b) were developed by Halperin,[13] Marques et al.,[14] Semenov,[15] and Birshtein and Zhulina.[16] In a third approach, van Lent and Schuetjens[17] used a self-consistent field theory to determine the detailed segment density profiles within a micelle, making no *a priori* assumptions as to the locations of the micellar components. The micelle structures determined

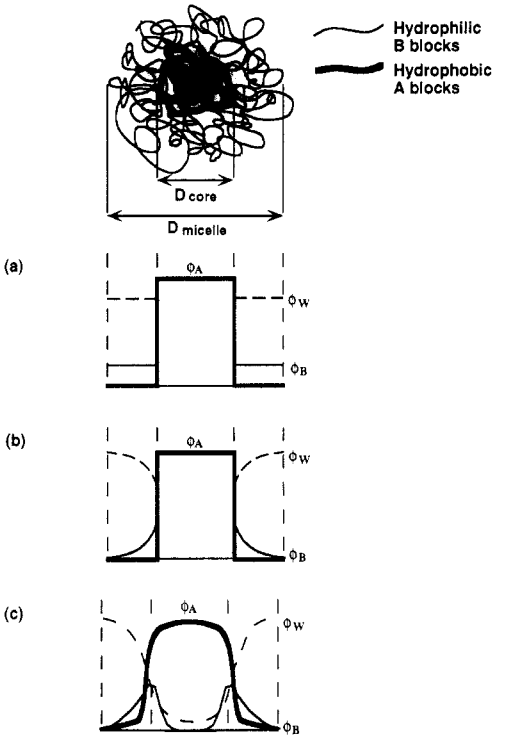

Figure 1. Schematic representation of the segment density profiles for the micellar components for the models of (a) Leibler et al.,[9] Noolandi and Hong,[10] and Nagarajan and Ganesh,[12,19] (b) Halperin,[13] and (c) van Lent and Scheutjens.[17] ϕ_A, ϕ_B, and ϕ_W are the volume fractions of segments A and B and of solvent, respectively.

from this model, illustrated schematically in Figure 1c, have been confirmed recently by Monte Carlo simulations[18] and show that the interfacial region between the core and corona of the micelle is diffuse, and not sharp as is assumed in the other modeling approaches.

The solubilization of solutes in these micellar systems has received significantly less attention theoretically. In the only known study, Nagarajan and Ganesh[19] extended their theory of micellization to describe solubilization in A–B diblock copolymer micelles. A spherical micelle was assumed, with a core consisting of solvent-incompatible A-blocks and solute and a corona which contained solvent and the solvent-compatible B-blocks. No allowance was

* Author to whom all correspondence should be addressed.
† Massachusetts Institute of Technology.
‡ Wageningen Agricultural University.
§ Deceased August 2, 1992.
® Abstract published in *Advance ACS Abstracts*, September 1, 1993.

0024-9297/93/2226-5592$04.00/0

made for solute molecules in the corona of the micelle, which leads trivially to their conclusion that "almost all" of the solute was confined to the core. Constant compositions of all components were assumed in both the core and the corona. The interfacial free energy was related to the interfacial tension between the core components and water, assuming a sharp interface between them and neglecting the presence of the B-blocks in the corona. The total free energy of solubilization was assumed to be due to contributions from the change in the state of dilution and deformation of the A-blocks in the core and of B-blocks in the corona, the localization of the joints between the blocks at the interface, and the free energy of the core–corona interface. By correlating their numerical results, Nagarajan and Ganesh found that for a PEO–PPO block copolymer in water, with benzene as the solubilizate, the micelle radius scales as $N_A^{0.92}N_B^{-0.13}$ and the volume fraction of benzene in the core scales as $N_A^{0.17}N_B^{-0.017}$. This latter trend with N_B for constant N_A is much weaker than that observed experimentally for the solubilization of polycyclic aromatics.[8]

A limitation of models of this type is that they assume *a priori* the aggregate structural features, and, as they do not explicitly account for polymer architecture (e.g., whether linear or branched, diblock or triblock, etc.), they cannot capture the finer details of the micelle structure and solubilizing characteristics. The self-consistent mean-field lattice theory of Scheutjens and Fleer,[20] on the other hand, is well suited to analysis of the solution behavior of association colloids, as is evident from the many studies on colloidal systems using this approach, which include homopolymer and block copolymer adsorption on surfaces,[17,20,21] interactions between adsorbed polymer layers,[22] and the formation of micelles,[23] vesicles,[24] and membranes.[25,26] For aggregation structures, the detailed segment density profiles are obtained, and macroscopic quantities such as the critical micelle concentration (cmc), aggregation number, and micelle size can be calculated. An extension of this theory to account for solubilization in block copolymer micelles formed by linear and starlike block copolymers is described in this paper, and the predictions of this theory are compared to the experimental results obtained by Hurter and Hatton.[8]

Theory

The Scheutjens–Fleer theory is an extension of the Flory–Huggins analysis of homogeneous polymer solutions,[27] in which the polymer chains are allowed to assume different conformations on a lattice. In the Flory–Huggins analysis, a first-order Markov approximation is used, so that the position of a segment depends only on that of the preceding segment in the chain, the result being that the chain conformation follows the path of a random walk. In addition, a mean-field assumption is invoked to describe the interactions between unlike segments. The free energy of the system is minimized to calculate the equilibrium thermodynamic properties of the polymer solution.

For spatially inhomogeneous systems such as those containing interfaces, Scheutjens and co-workers[17,20,23] restricted the mean-field approximation to two dimensions, i.e., within parallel or concentric lattice layers, and applied a step-weighted random walk to account for the inhomogeneities normal to the layers. The polymer and solvent molecules are assumed to be distributed over a lattice such that solvent molecules and polymer segments occupy one lattice site each. Each polymer chain can assume a large number of possible conformations, defined by the layer numbers in which successive segments are found. There

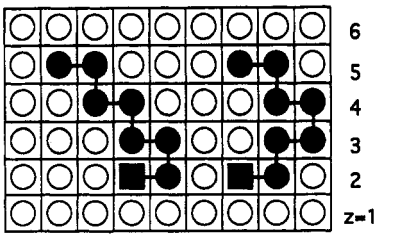

Figure 2. Two possible arrangements of a polymer with the same conformation on a planar lattice.

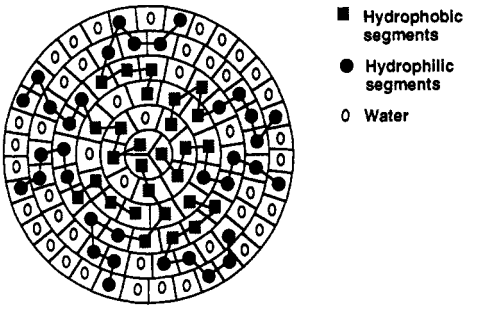

Figure 3. Schematic representation of a spherical lattice. The amphiphilic molecules assume various conformations to form a micelle.

can be many different arrangements for each conformation; Figure 2 shows two such arrangements for a planar geometry. If the number of polymer chains in each conformation is specified, the configurational entropy contribution to the system free energy can be evaluated, the other contributions to this free energy being due to the interactions between the polymer molecules, solvent molecules, and the surface, which are characterized by Flory–Huggins χ-parameters. If the free energy of the system is minimized with respect to the number of polymer chains in each conformation, it is possible to calculate the equilibrium segment density profiles. The self-consistent field theory can be used to calculate the segment density profiles in a micelle once the aggregation number of the micelle is known.[17,23,24] To find this aggregation number, small-system thermodynamics can be used,[28-30] in which the change in the free energy due to the change in the number of micelles (at constant temperature, pressure, and number of molecules) must be zero at equilibrium. This "excess free energy" is the sum of the energy required to create micelles and the energy due to the translational entropy of the micelles. Since the segment density profiles are required to calculate the energy of micelle formation, an iterative process is required.

In this section we summarize the details of this theory, extend it to the case of symmetrically-branched block copolymers, and allow for the presence of solubilizates.

Generation of the Lattice. For spherical micelles, a curved lattice such as that illustrated in Figure 3 is used. The number of lattice sites in each layer (which increases with z and is not necessarily an integral number) can be generated mathematically, as described below. It is assumed that all lattice sites have equal volumes and that all lattice layers are equidistant. The layers are numbered from the center of the micelle ($z = 1$) toward the bulk solution ($z = M$). The volume $V(z)$ of a lattice with z layers (in number of lattice sites) is given by

$$V(z) = {}^4/_3\pi z^3 \tag{1}$$

The number of lattice sites in layer z is

$$L(z) = V(z) - V(z-1) \tag{2}$$

The contact area between layers z and $z + 1$, $S(z)$, is

$$S(z) = 4\pi z^2 \tag{3}$$

The fraction of contacts that a lattice site in layer z has with sites in layers $z + 1$, z, and $z - 1$ is given by λ_{+1}, λ_{-1}, and λ_0, respectively. It is clear that

$$\lambda_{-1}(z) + \lambda_0(z) + \lambda_{+1}(z) = 1 \tag{4}$$

The number of possible steps from layer z to layer $z + 1$ must be equal to the number of steps from layer $z + 1$ to layer z, so that

$$ZL(z)\,\lambda_{+1}(z) = ZL(z+1)\,\lambda_{-1}(z+1) \tag{5}$$

where Z is the coordination number of the lattice. The fraction of possible contacts between two layers should be proportional to the contact area $S(z)$, which determines the fraction of contacts a site in layer z has in the neighboring layers:

$$\lambda_{-1}(z) = \lambda S(z-1)/L(z) \tag{6}$$

$$\lambda_{+1}(z) = \lambda S(z)/L(z) \tag{7}$$

where λ is the transition probability for a planar lattice in the bulk solution. In these calculations, a hexagonal lattice is used, so that $\lambda = {}^1/_4$ and $\lambda_0 = {}^1/_2$.

Segment Density Distributions. To generate the chain conformations, a step-weighted random walk is used. The total potential experienced by a segment of type A in layer z, $u_A(z)$, has two contributions, the hard-core potential and the energy of interaction. The hard-core potential $u'(z)$ is independent of segment type and satisfies the assumption of constant density in a layer.[23] The interaction energy accounts for the heat of mixing between unlike segments. In the mean-field approximation, the exact location of segments within a layer is not known, and average volume fractions within the layer are used to calculate the energy of interaction. The potential is thus composition-dependent and is given by

$$u_A(z) = u'(z) + kT\sum_B \chi_{AB}(\langle\phi_B(z)\rangle - \phi_B^{\infty}) \tag{8}$$

where $\phi_B(z)$ and ϕ_B^{∞} are the volume fractions of segment type B in layer z and in the bulk solution, respectively, and the angular brackets indicate an averaging of the volume fraction over three layers, so that

$$\langle\phi_B(z)\rangle = \lambda_{-1}(z)\,\phi_B(z-1) + \lambda_0(z)\,\phi_B(z) + \lambda_{+1}(z)\,\phi_B(z+1) \tag{9}$$

The Flory–Huggins interaction parameter χ_{AB}[27] is used to characterize the interaction between unlike segment types. The free segment weighting factor $G_A(z)$, which is proportional to the probability of finding an unconnected segment of type A in layer z, is given by the Boltzmann factor containing the local potential experienced by the segment

$$G_A(z) = \exp[-u_A(z)/kT] \tag{10}$$

The volume fraction of a monomeric segment A in layer z would be given by

$$\phi_A(z) = \phi_A^{\infty} G_A(z) \tag{11}$$

To calculate the volume fraction profiles of polymeric molecules, the chain connectivity must be taken into account. The notation used is that $G(z,s|z',s')$ is the weighting factor for the probability of finding segment s in layer z, given that segment s' is in layer z'. A matrix of end-point distribution functions can be generated, where

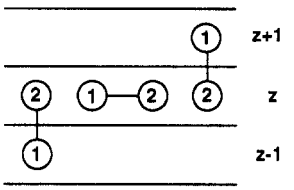

Figure 4. Conformations available to a dimeric molecule which terminates the random walk with the end segment in layer z.

$G(z,s|1)$ is the probability of segment s being in layer z, for a walk starting with segment 1 in any layer and ending in segment s. Clearly, the probability of a monomer being found in layer z is equal to the free segment weighting factor, so that

$$G(z,1|1) = G(z) \tag{12}$$

The situation for dimeric molecules is illustrated in Figure 4. The probability of finding the end segment (segment 2) in layer z is the product of the probability of finding segment 2 in layer z, which is $G(z)$, and the probability of finding segment 1 in layer $z - 1$, layer z, or layer $z + 1$, which is given by $\langle G(z)\rangle = \langle G(z,1|1)\rangle$. Hence

$$G(z,2|1) = [\lambda_{-1}(z)\,G(z-1,1|1) + \lambda_0(z)\,G(z,1|1) + \lambda_{+1}(z)\,G(z+1,1|1)]\,G(z) = \langle G(z,1|1)\rangle G(z) \tag{13}$$

where once again the angular brackets have been used to indicate a weighted average over the three layers. For s-mers, a recurrence relation can be developed, and a matrix of end-point distributions can be generated for a polymer with r segments in a lattice with M layers:

$$\begin{bmatrix} G(1,1|1) & \cdots & G(1,r|1) \\ \cdots & & \cdots \\ G(z,1|1) & \cdots\ G(z,s|1)\ \cdots & G(z,r|1) \\ \cdots & & \cdots \\ G(M,1|1) & \cdots & G(M,r|1) \end{bmatrix}$$

where

$$G(z,s|1) = \langle G(z,s-1|1)\rangle G(z) \tag{14}$$

In an analogous manner, a matrix of end-point distributions assuming that segment r is free can also be generated, i.e., a matrix of $G(z,s|r)$.

The statistical weight of all conformations with segment s in layer z, given that segment $s = 1$ and segment $s = r$ are free, denoted $G(z,s|1;r)$, is the product of three terms: the probability of finding segment $s - 1$ in layer z, $z - 1$, or $z + 1$ given that segment 1 is free, the probability of finding segment $s + 1$ in layer z, $z - 1$, or $z + 1$ given that segment r is free, and the probability of finding a free segment s in layer z:

$$G(z,s|1;r) = \langle G(z,s-1|1)\rangle G(z)\langle G(z,s+1|r)\rangle \tag{15}$$

But since

$$\langle G(z,s-1|1)\rangle = G(z,s|1)/G(z); \quad \langle G(z,s+1|r)\rangle = G(z,s|r)/G(z) \tag{16}$$

the expression for $G(z,s|1;r)$ becomes

$$G(z,s|1;r) = \frac{G(z,s|1)\,G(z,s|r)}{G(z)} \tag{17}$$

The volume fraction of segment s in layer z is clearly proportional to $G(z,s|1;r)$:

$$\phi(z,s) = cG(z,s|1;r) \tag{18}$$

To find the proportionality constant, the total amount of polymer in the system, θ, is introduced:

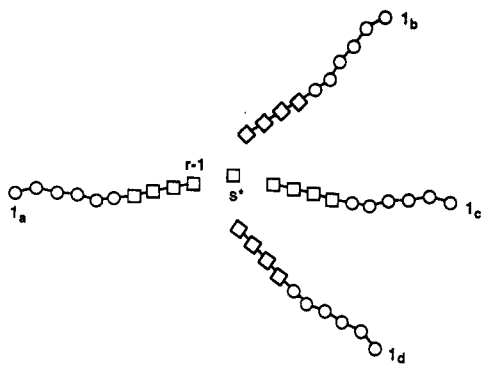

Figure 5. Schematic representation of a starlike molecule.

$$\theta = \sum_{z=1}^{M}\sum_{s=1}^{r}\phi(z,s) = r\sum_{z=1}^{M}\phi(z,r) = cr\sum_{z=1}^{M}G(z,r|1) \quad (19)$$

$$c = \frac{\theta}{rG(r|1)} \quad \text{where} \quad G(r|1) = \sum_{z=1}^{M}G(z,r|1) \quad (20)$$

In this derivation, use has been made of the fact that the total number of polymer segments in the system is r times the amount of a single segment.

The derivation above was for the simple case of a linear homopolymer. For heterogeneous polymers, $G(z)$ is replaced by $G_A(z)$, which is the free segment weighting factor for a segment of type A. The end-point distribution matrices are generated for each molecule in the system.

We now consider a symmetrically branched molecule, such as that illustrated in Figure 5, with b branches of length $r - 1$ segments connected by segment s^*. The probability of finding segment s^* in layer z is given by

$$G(z,s^*|1_a;1_b;1_c...) = \langle G(z,r-1|1)\rangle G(z)\langle G(z,r-1|1)\rangle^{b-1} \quad (21)$$

It can be shown that this expression reduces to

$$G(z,s^*|1_a;1_b;1_c...) = \frac{G(z,r|1)^b}{G(z)^{b-1}} \quad (22)$$

and eq 18 can be used to find the volume fraction of the segment s^*. Making use of the symmetry of the molecule, one only needs to compute the segment density contribution of the segments $s = 1, ..., r_a - 1$ and multiply the results with the number of branches b. Thus the total volume fraction of all segments s in layer z, for all branches, is then given by

$$\phi = cbG(z,s|1_a;1_b;1_c...) \quad (23)$$

where c is a normalization constant similar to that given in eq 20 and

$$G(z,s|1_a;1_b;1_c...) = (G(z,s|1_a)\,G(z,s|1_b;1_c;...))/G(z) \quad (24)$$

The chain end distribution $G(z,s|1_b;1_c;...)$ is computed starting from $G(z,s^*|1_b;1_c;...)$ and using the recurrence relation as given in eq 14 $s^* - s$ times. Finally, similar to eq 22

$$G(z,s^*|1_b;1_c;...) = (G(z,s^*|1_a)^{b-1})/G(z)^{b-2} \quad (25)$$

Computational Aspects. An iterative procedure is required for calculating the volume fraction profiles, since the interaction energy is composition-dependent. An initial guess is made for the potentials $u_A(z)$, which allows the volume fraction profiles to be calculated. The potentials are then updated. The iteration is carried out using a modified Newton method. The computer code written to perform these calculations is capable of predicting the formation of spherical micelles and planar membranes for starlike symmetric molecules with any number of branches and linear molecules. An object-oriented programming language, Simula, was used, which is particularly well suited to molecular simulations. The calculations were performed on a Sun SPARCstation 2 (Sun Microsystems). Owing to the matrix technique used to generate the polymer conformations, the computation time is very rapid, with each calculation taking of the order of 1 min of computer time.

Small-System Thermodynamics. Hall and Pethica[31] used the small-system thermodynamics approach of Hill[29,30] to study the free energy of micelle formation. It is assumed that each micelle occupies one small system of volume V_s. It can be shown that the total free energy of a system containing $\mathcal{N}$ small systems is given by

$$dF_t = -S_t\,dT + V_t\,dP + \sum_i \mu_i\,dN_{t,i} + \epsilon\,d\mathcal{N} \quad (26)$$

where S_t is the total entropy, V_t is the total volume, T is the temperature, P is the pressure, μ_i is the chemical potential of component i, $N_{t,i}$ is the total number of molecules of i, and ϵ is the subdivision potential, which is the energy required to subdivide the system to form another micelle. For a closed ensemble of open systems at equilibrium, the free energy is a minimum, which leads to the following equilibrium conditions:

$$\epsilon = 0 \quad (27)$$

$$\partial\epsilon/\partial\mathcal{N} > 0 \Rightarrow \partial\epsilon/\partial n_{agg} < 0 \quad (28)$$

where n_{agg} is the aggregation number of the micelle. The subdivision potential is equal to the overall excess free energy of micelle formation. In the self-consistent field theory, the excess free energy of micelle formation is calculated for a micelle with a center of mass fixed in the coordinate system. Consequently, entropy terms which account for the translational freedom of the center of mass have to be added, so that

$$\epsilon = A^\sigma + kT\ln\frac{V_m}{V_s} = 0 \quad (29)$$

where A^σ is the translationally restricted excess free energy of micelle formation, V_m is the volume of the micelle, and V_s is the small-system volume (which is the total volume divided by the number of micelles, i.e., the volume that is occupied by a single micelle with its accompanying bulk solution). This is very similar to the analysis of Leibler et al.[9] where the total free energy of the system is composed of the free energy of micelle formation plus contributions from the translational entropy of the micelles and the free copolymer molecules in solution.

By minimizing the grand canonical partition function for one micelle with fixed center of mass, one can derive an expression for A^σ:[23]

$$A^\sigma = -\sum_{i=1}^{c}\frac{\theta_i^{exc}}{r_i} - \sum_{z=1}^{M}L(z)\,u'(z) - \frac{1}{2}\sum_A\sum_B\sum_{z=1}^{M}\chi_{AB}L(z)[\phi_A(z)\langle\phi_B(z)\rangle - \phi_A^\infty\phi_B^\infty] \quad (30)$$

where the third term is a summation over all segment types and θ_i^{exc} is the excess number of segments of molecule

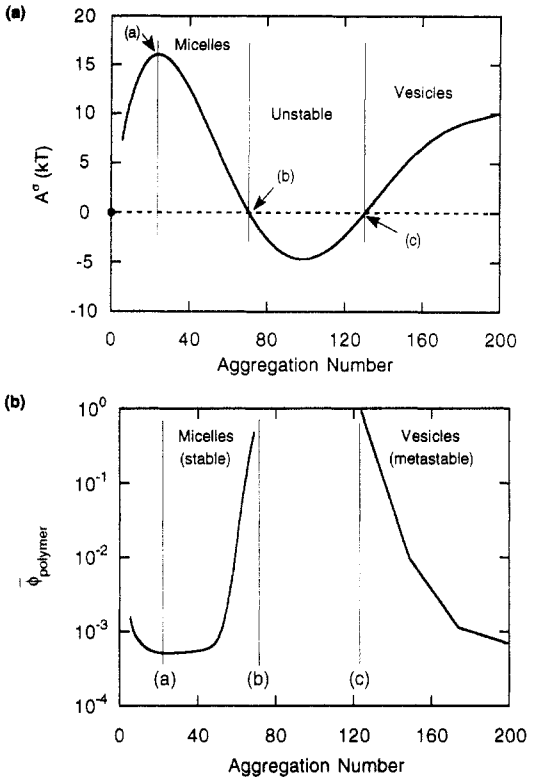

Figure 6. (a) A characteristic stability curve, which shows the translationally restricted excess free energy of micelle formation as a function of aggregation number. (b) Polymer composition as a function of the aggregation number for micelles and vesicles.

i in the small system, compared to the bulk solution, which is given by

$$\theta_i^{exc} = \sum_{z=1}^{M} \sum_{s=1}^{r} L(z)[\phi_i(z,s) - \phi_i^{\infty}] \quad (31)$$

Once the aggregation number is specified, the volume fraction profiles can be calculated using the matrix technique outlined in the previous section, and hence the volume of the micelle can be found by examining the micellar profiles. Equation 30 can be used to calculate A^σ, after which the volume of the small system can be found from the equilibrium expression in eq 29. The average composition of each component in the system, $\bar{\phi}_i$, can then be calculated since

$$\bar{\phi}_i = \theta_i^{exc}/V_s + \phi_i^{\infty} \quad (32)$$

The second equilibrium condition, eq 27, which ensures that the equilibrium is stable, becomes

$$\partial A^\sigma/\partial n_{agg} < 0 \quad (33)$$

If A^σ is calculated as a function of aggregation number, a characteristic stability curve is obtained, as illustrated in Figure 6a. At very low aggregation numbers, no numerically stable results are obtained other than a homogeneous solution, indicating that no micelles are formed. As the aggregation number is increased, micelles form, but these are metastable since eq 33 is not satisfied. The maximum in the figure at point a indicates the onset of stable micelles; the polymer composition at which this occurs corresponds to the critical micelle concentration. Between points a and b, stable micelles form, with the average concentration of polymer increasing as the aggregation number increases. Point b, where A^σ is zero, corresponds to a polymer composition of unity. A^σ becomes positive again at point c, and beyond this point the aggregate profiles indicate that metastable vesicles are formed. No aggregative structures can form having aggregation numbers in the region between points b and c, where A^σ is negative.

Figure 6b shows the aggregation number of the micelles as a function of average polymer composition. Close to the critical micelle concentration, the aggregation number changes rapidly with polymer concentration; however, at higher polymer concentrations, the aggregation number is significantly less sensitive to changes in $\phi_{polymer}$.

Table I. Sources and Values of the χ-Parameters Used in the Calculations

components	χ_{AB}	source of data	ref
PEO–water	0.4	vapor pressure	34
PPO–water	2.0	vapor pressure	34
benzene–water	5.5	aqueous solubility of PAHs, χ from Flory's phase equations	35, 27
PEO–benzene	0.14	vapor pressure	36
PEO–PPO	0.006	interfacial tension, using scaling relation for $\gamma = f(\chi)$	37, 38
benzene–PPO	0.1	estimated to be between zero and $\chi_{PEO,B}$	

Table II. Molecular Volumes of the Segments[a]

component	molecular vol (Å^3)	component	molecular vol (Å^3)
water	30	benzene (in naphthalene)	104
EO	62	benzene (in phenanthrene)	89
PO	96	benzene (in pyrene)	71

[a] Data are derived from molar volumes reported by May et al.[35]

Parameter Evaluation. For the system of PEO–PPO block copolymers in water, with PAH solutes, six Flory–Huggins interaction parameters are required. These have been obtained from the literature, either directly or indirectly by analyzing relevant data. Table I shows the χ-parameters used in this study and the source of the data. It must be emphasized that none of these parameters was curve-fitted to the solubilization data and that they were all obtained independently and then used to predict the solubilization of PAHs in PEO–PPO block copolymer micelles.

The χ-parameters for PEO–W and PPO–W are found empirically to be dependent on the composition of the solute and are not simply inversely proportional to temperature, as implicit in the original formulation of the Flory–Huggins theory. As a first approximation, we have assumed that χ is independent of composition. In a later paper,[32] a model will be presented which accounts for the temperature and composition dependence of the interactions in a physically realistic manner.

For simplicity and to avoid the introduction of additional parameters, it was assumed that each segment of PPO, PEO, or benzene and each water molecule occupied one lattice site. Table II lists the molecular volumes of these components, which shows that they are at least of the same order of magnitude. It must be recognized, however, that differences in the monomer, solute, and solvent shapes and sizes will be important in determining detailed micellization behavior, and thus the predictions afforded by our model calculations must be viewed primarily as being qualitative in nature rather than quantitative, although a semiquantitative predictive ability should not be ruled out. By the same token, the delicate issue concerning the correspondence between the polymerization degrees used in the numerical studies and the molecular weights of the real polymers (a lattice site corresponds to a Kuhn length rather than to the individual monomer sizes as used here) also reduces the quantitative reliability of our predictions. Nevertheless, the model is

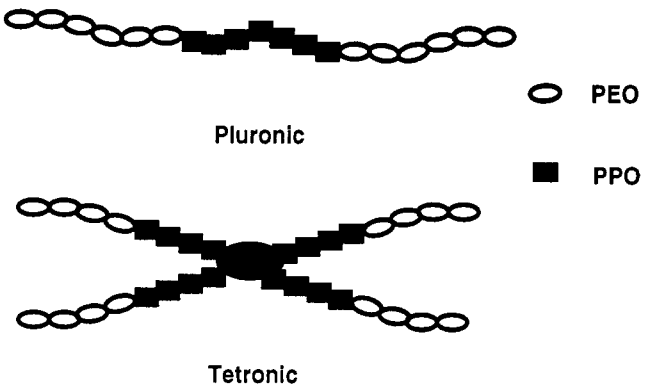

Figure 7. Structure of the BASF Pluronic and Tetronic polymers.

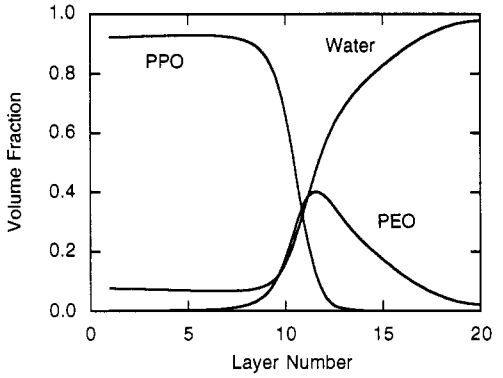

Figure 8. Segment density profiles of a micelle formed by a linear triblock copolymer. Layer number 1 corresponds to the center of the micelle, and layer 20 is approaching the bulk solution. The PPO forms a dense, hydrophobic core, which is shielded from the water by a hydrophilic corona of PEO segments.

Table III. Molecular Structures of Simulated Polymers

BASF polymer	PEO content (wt %)	mol wt (Da)	polymer structure
P103	30	4950	$(EO)_{20}(PO)_{61}(EO)_{20}$
P104	40	5900	$(EO)_{30}(PO)_{61}(EO)_{30}$
P105	50	6500	$(EO)_{42}(PO)_{61}(EO)_{42}$
F108	80	14600	$(EO)_{168}(PO)_{61}(EO)_{168}$
P123	30	5750	$(EO)_{21}(PO)_{69}(EO)_{21}$
P84	40	4200	$(EO)_{19}(PO)_{43}(EO)_{19}$
L64	40	2900	$(EO)_{13}(PO)_{29}(EO)_{13}$
T904	40	6700	$((EO)_{16}(PO)_{17})_4PO$
T1304	40	10500	$((EO)_{25}(PO)_{27})_4PO$
T1504	40	12000	$((EO)_{39}(PO)_{31})_4PO$
T1107	70	15000	$((EO)_{62}(PO)_{19})_4PO$
T1307	70	18000	$((EO)_{75}(PO)_{23})_4PO$

useful for the semiquantitative interpretation of the trends described by Hurter and Hatton,[8] which was the primary goal of this work.

Results

Aggregates Formed by Pluronic and Tetronic Polymers. The micellar profiles and solubilizing capacity of both linear and branched molecules were investigated in this work. The polymers modeled were based on the Pluronic and Tetronic block copolymers manufactured by BASF Corp., which have poly(ethylene oxide) (PEO) as the hydrophilic part and poly(propylene oxide) (PPO) as the hydrophobe. The Pluronics are linear triblock copolymers with the hydrophobic block in the center of the molecule, while the starlike Tetronic polymers have four arms. The structures of these polymers are illustrated schematically in Figure 7. Their properties are listed in Table III.

Figure 8 shows the volume fraction profiles of a micelle formed by a Pluronic polymer with 30 wt % PPO. Most

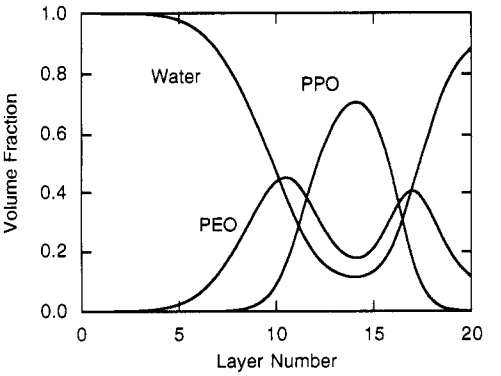

Figure 9. Segment density profiles for a metastable vesicle formed by a branched, Tetronic block copolymer. Layer 1 is at the center of the vesicle.

macroscopic theories of micelle formation[9-12] assume that there is a micelle core which contains only hydrophobic segments, that the corona is composed of hydrophilic segments and water, with a uniform concentration profile, and that there is a sharp interface between the core and corona. These more detailed calculations indicate that there is a finite, though small, concentration of water in the core and that there is a diffuse interface between the core and the corona and between the corona and the bulk solution. These effects could become particularly important when dealing with the solubilization of molecules that favor the interfacial region. The water content of the core region is probably overpredicted, as no allowance is made for bulk water structure in the model, which would lead to a lower propensity for water to enter the more confined core.

At large aggregation numbers, the theory predicts the formation of metastable vesicles, as has also been observed by Leermakers and Scheutjens[24] for lipid molecules. The volume fraction profiles for a vesicle formed by a Tetronic molecule are illustrated in Figure 9. Again, there is a finite water content within the apolar regions, and the interface is diffuse. Since these structures are metastable, they are not expected to occur in real systems, however.

The characteristic stability curves for Pluronic and Tetronic molecules are compared in Figure 10. Figure 10a shows the results for molecules with a total molecular weight of 121 segments, with equal numbers of hydrophilic and hydrophobic segments. Both molecules form micelles throughout the composition range, though the Pluronic polymers give higher aggregation numbers. For lower molecular weight polymers, with a total molecular weight of 81 segments (Figure 10b), it would seem that the Tetronic molecules cannot form micelles at most polymer concentrations; the minimum in the figure, which represents the upper limit for spherical micelle formation, actually corresponds to a polymer volume fraction of 10^{-4}. This suggests that other surfactant phases (for example an interacting lamellar phase) are preferred at higher concentrations. The Pluronic molecules once again form micelles at all concentrations above the critical micelle concentration. The branched structure of the Tetronic micelle probably makes micelle formation less favorable due to steric hindrance. Figure 10 shows that the critical micelle concentration (cmc) is lower for Pluronic than Tetronic micelles, since A^σ is higher at the critical point; eq 29 indicates that a higher A^σ leads to a lower polymer concentration for the same micelle size, since V_s must increase.

The segment density profiles of micelles formed by Pluronic and Tetronic molecules are compared in Figure 11. As the branched Tetronic molecules are less flexible

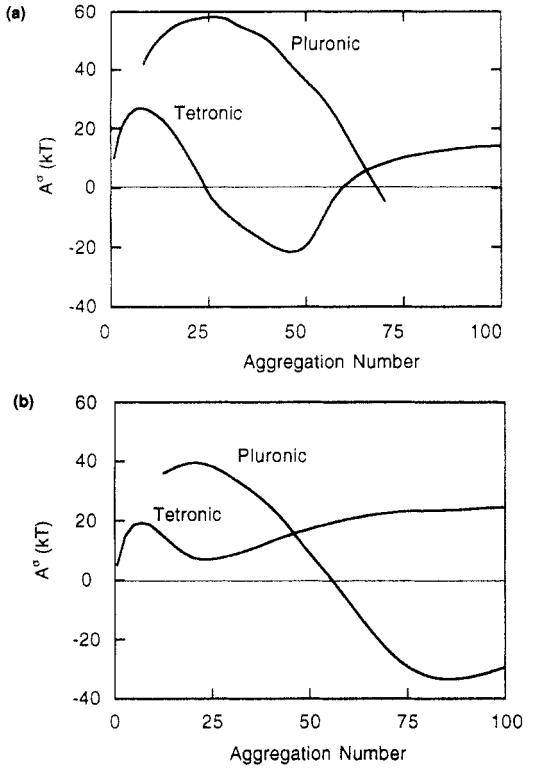

Figure 10. Stability curves for Pluronic and Tetronic polymers with PEO:PPO molar ratios of unity. Total polymer molecular weight of (a) 121 segments and (b) 81 segments.

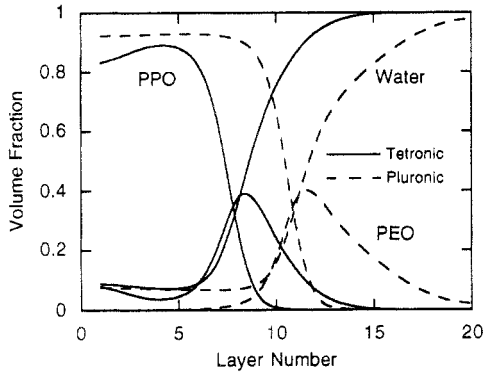

Figure 11. Comparison of the segment density profiles of micelles formed by Pluronic and Tetronic polymers. The Tetronic polymers form smaller micelles, with a lower concentration of PPO in the core.

than the linear Pluronics, particularly at low molecular weight, steric hindrance in the core of the micelle leads to the Tetronic polymers forming a "looser" structure with a lower concentration of PPO and a higher concentration of PEO in the core, i.e., a higher degree of mixing of PEO and PPO segments in this region. The Tetronic micelle is also smaller than the Pluronic micelle, as anticipated based on its lower aggregation number (see Figure 10).

Solubilization of Naphthalene. Naphthalene was modeled as a chain molecule consisting of two benzene rings. Figure 12a shows the segment density profiles for naphthalene solubilized within a block copolymer micelle. The solute is confined chiefly to the core of the micelle, as is illustrated more clearly in Figure 12b, which shows the ratio of naphthalene to polymer concentrations in the micelle. The amount of naphthalene solubilized falls off sharply after about the tenth layer, which corresponds to the radius of the homogeneous core region in Figure 12a. Significantly less naphthalene is solubilized within the interfacial region. Note that even within the homogeneous core region, the naphthalene concentration falls as the

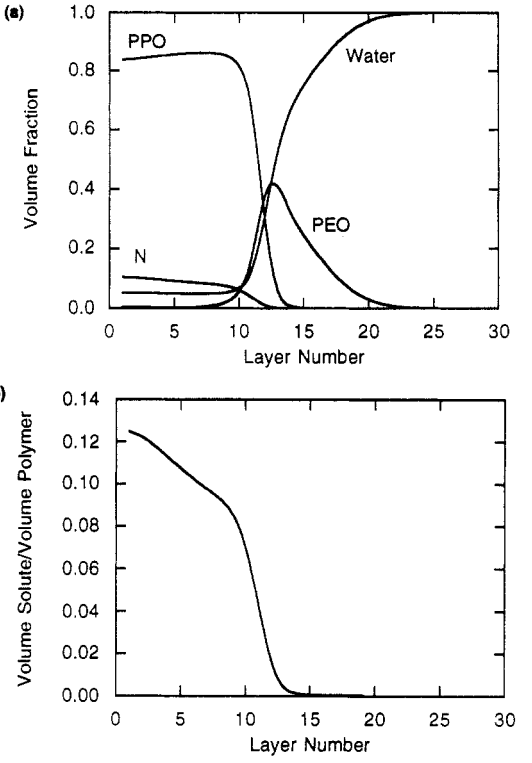

Figure 12. (a) Segment density profiles for naphthalene solubilized within a micelle formed by P104, a Pluronic polymer with 60 wt % PPO. The polymer concentration is 2%, and the volume of naphthalene in the bulk is 1×10^{-5}. The curve for naphthalene is labeled N. (b) Ratio of naphthalene to polymer concentration in the micelle. The naphthalene is solubilized mainly within the core of the micelle.

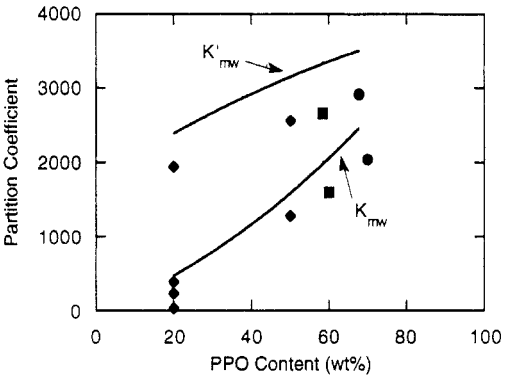

Figure 13. Effect of PPO content of a linear triblock copolymer on the micelle–water partition coefficient of naphthalene. The experimental results are from Hurter and Hatton,[8] and the theoretical results are indicated by the solid line.

corona region is approached. This is because the solute molecules near the interfacial region are more restricted in their possible orientations since some conformations will result in unfavorable solute/EO segment and solute/water contacts. Thus, for the same overall composition of the micellar phase, smaller micelles will lead to lower overall solubilization capacities. This conclusion is borne out by the results discussed below. In Figure 13, the experimental results of Hurter and Hatton[8] for the micelle–water partition coefficient, K_{mw}, of naphthalene solubilized in aqueous solutions of Pluronic polymers are compared with calculated results. The partition coefficient is defined as

$$K_{mw} = c_s^m / c_s^w \tag{34}$$

where c_s^m and c_s^w are the concentrations of the solute in the micelle and in the water, respectively. The polymers used in this experiment all had the same molecular weight

of PPO (approximately 3500 Da) but varied in the size of the PEO block. The experimental results show a strong effect of the polymer composition on naphthalene partitioning, as the more hydrophobic the polymer becomes, the greater is the micelle–water partition coefficient; this is reproduced by the theory. The strong correlation between the PPO content of the polymer and the partition coefficient is reasonable since one would expect naphthalene, which is extremely hydrophobic and has a water solubility of only 3×10^{-2} g/L,[33] to associate with the PPO segments and to solubilize within the core of the micelle. However, the effect is not solely due to the change in the relative amount of PPO in the polymer. If the partition coefficient is defined in terms of a concentration based on the PPO content of the polymer solution and not on the total polymer concentration, then we obtain the modified partition coefficient $K'_{mw} = K_{mw}/f_{PPO}$, where f_{PPO} is the mass fraction of PPO in the polymer. The fact that K'_{mw} is not constant indicates that some factors other than simply the PPO content of the polymer must be contributing to the solubilization of the naphthalene in the micelles. The positive slope of the curve suggests that this effect is not due to association with the EO groups,[8] a conclusion that is consistent with the predicted profiles shown in Figure 12, which indicate no association of the solute with the EO groups in the corona. Rather, this effect is the result of the changing structure of the micelles as the fraction of PPO in the polymer increases, as intimated above. Indeed, it is clear from Figure 14a that for constant PPO block size, an increase in PEO block length (or decrease in PPO fraction) results in a smaller micelle core, while the corona becomes more extended. This is reflected in the decreasing aggregation number for the micelles shown in Figure 14b. As stated above, smaller micelles will lead to lower overall solubilization capacities because of the increasing importance of the interfacial region relative to the core interior; these results are consistent with the experimental trends noted above.

Figure 15 shows the experimental results of Hurter and Hatton[8] for the micelle–water partition coefficient of naphthalene as a function of molecular weight of the polymer. Here the agreement between model predictions and experimental results is not as encouraging as before. While the observed effect of K_{mw} increasing with increasing molecular weight is reproduced qualitatively for both the Tetronic and Pluronic molecules, the experimental results show a far larger dependence of K_{mw} on molecular weight. Calculations similar to those shown in Figure 14 indicate that higher molecular weight polymers of constant composition ratio form larger micelles, which results in a decrease in the interfacial volume compared to the core volume. Since naphthalene is effectively excluded from the interfacial region (Figure 12), larger micelles should give rise to higher micelle–water partition coefficients. Not taken into account in these calculations is the composition dependency of the Flory–Huggins χ-parameters, and it is shown in a subsequent paper[32] that incorporation of these effects gives the strong molecular weight dependence observed experimentally.

The theoretical calculations agree with the experimental finding that naphthalene partitions more favorably into the linear Pluronic polymers than into the branched Tetronic molecules. As is illustrated in Figure 11, the Tetronics form micelles with a lower concentration of PPO in the core, resulting in a less hydrophobic core environment, which would inhibit naphthalene solubilization. In addition, the Tetronic molecules form smaller micelles, which is expected to result in a lower micelle–water partition coefficient because of the changing ratio of bulk versus interfacial region distribution of the PO segments.

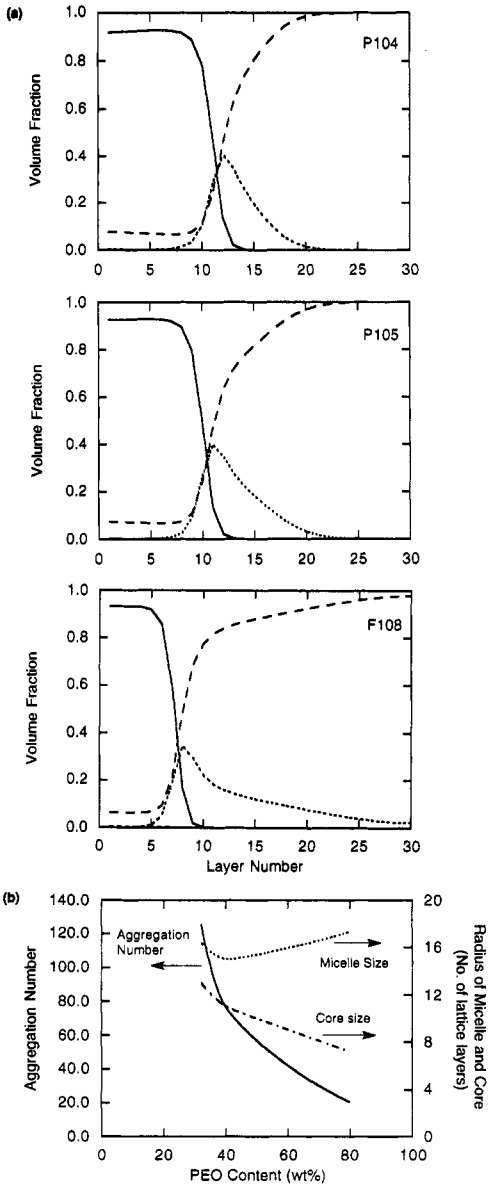

Figure 14. Effect of the PEO block length on the segment density profiles for water, PPO, and PEO, and the effect of PEO content on the aggregation number and core and total micelle size.

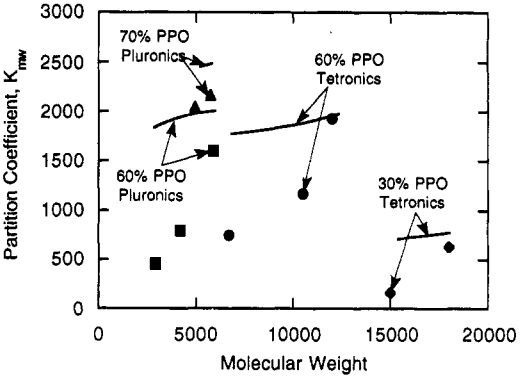

Figure 15. Effect of polymer molecular weight on the micelle–water partition coefficient of naphthalene. The experimental results are from Hurter and Hatton,[8] while the theoretical predictions are indicated by the solid lines.

The self-consistent mean-field analysis used in this work is thus able to reproduce the experimental observation that polymer structure, composition, and molecular weight all play a role in determining the solubilization behavior

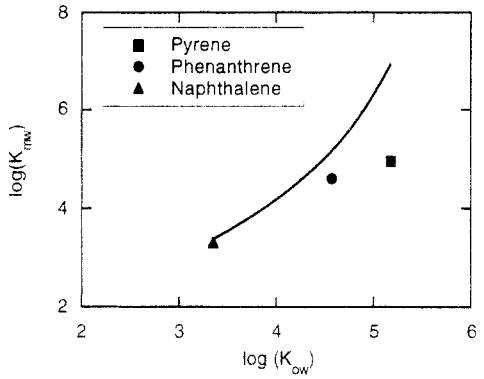

Figure 16. Micelle–water partition coefficients of naphthalene, phenanthrene, and pyrene, solubilized in a Pluronic polymer with 70% PPO, plotted as a function of the solute octanol–water partition coefficients. The solid line represents the theoretical results, and the experimental results are from Hurter and Hatton.[8]

of naphthalene in micelles formed by these polymers. Since polymer structure has an effect on the properties of the micelle formed, this implies that the detailed micelle structure, and not just the amount of polymer in the system, is important in determining solubilization behavior.

Solubilization of PAHs. Three PAHs (naphthalene, phenanthrene, and pyrene, composed of two, three, and four fused benzene rings, respectively) were modeled as chains of flexible benzene rings, and their fused nature and detailed structure were not taken into account. Figure 16 shows the correlation between the micelle–water partition coefficient of these three PAHs and the octanol–water partition coefficient, K_{ow}, which is a standard measure of hydrophobicity.

As anticipated, there is a strong correlation between K_{mw} and K_{ow}. This effect is due chiefly to the decrease in water solubility of the PAHs as the molecular weight is increased, as discussed by Hurter and Hatton.[8] The concentration of the solute in the micelle (on a weight basis) remains of the same order of magnitude and in fact decreases slightly with an increase in solute molecular weight. This seems reasonable since all solutes have approximately the same interaction energy per benzene ring, but the larger solutes might experience an entropic penalty from being confined to the micelle interior.

The theoretical results overpredict K_{mw} for the higher molecular weight solutes. This is not surprising, since the PAHs were modeled as flexible chain molecules, whereas they are actually composed of fused benzene rings. The model would thus have overpredicted the number of configurations available to the solutes in the micelle interior, which explains the higher theoretical value of K_{mw}. The detailed structure of the PAHs is clearly important. For example, phenanthrene and anthracene, which both have three fused benzene rings, have water solubilities which differ by a factor of 20. The simplifying assumptions made here preclude the possibility of predicting these second-order effects, which can also manifest themselves in the partitioning experiments.

Conclusion

The self-consistent field theory is a useful tool for investigating the properties of self-aggregating systems and their capacity for hosting solubilized molecules. In particular, it has been shown here that it is possible to elucidate the solubilization behavior of polycyclic aromatic hydrocarbons in poly(ethylene oxide)–poly(propylene oxide) block copolymers by providing detailed information on the microstructure of the micelles formed by linear and branched copolymers. The calculations showed qualitative agreement with experimental predictions on the effect of hydrophobicity and molecular weight of the polymer, and quantitative agreement was remarkably good considering that all parameters were obtained from independent experiments. Many of the speculations advanced by Hurter and Hatton[8] as to the reasons for the experimental observations have thus been confirmed.

While the theory presented here has been successful in predicting the solubilization behavior of PAHs in block copolymer micelles, it has overlooked the fact that, in general, the χ-parameters are found to be both composition and temperature dependent in ways different than stipulated in the original lattice theories for polymer solutions.[27] This limitation will be lifted in a later paper,[32] in which the polymer segments themselves are able to assume different conformations (grouped as polar and nonpolar) as a result of the trans and gauche rotations of the C–C and C–O bonds in the individual segments.

Acknowledgment. This work was funded primarily by the M.I.T. Sea Grant College Program, under Federal Grant No. NA90-AA-SG-D424 from the National Sea Grant College Program, from the National Oceanic and Atmospheric Administration, U.S. Department of Commerce. Additional funding was provided by Union Carbide as matching funds for an NSF Presidential Young Investigator Award to T.A.H. and by the Department of Energy under Grant No. DE-FG02-92ER14262. We would like to thank Frans Leermakers and Gerard Fleer as well as two anonymous reviewers for their critical reading of the manuscript and for some helpful suggestions on improving the clarity of this paper.

References and Notes

(1) Collett, J. H.; Tobin, E. A. *J. Pharm. Pharmacol.* **1979**, *31*, 174–177.
(2) Lin, S.-Y.; Kawashima, Y. *Pharm. Acta Helv.* **1985**, *60*, 339–344.
(3) Tontisakis, A.; Hilfiker, R.; Chu, B. *J. Colloid Interface Sci.* **1990**, *135*, 427–434.
(4) Nagarajan, R.; Barry, M.; Ruckenstein, E. *Langmuir* **1986**, *2*, 210–215.
(5) Nowakowska, M.; White, B.; Guillet, J. E. *Macromolecules* **1989**, *22*, 3903–3908.
(6) Nowakowska, M.; White, B.; Guillet, J. E. *Macromolecules* **1989**, *22*, 2317–2324.
(7) Sustar, E.; Nowakowska, M.; Guillet, J. E. *J. Photochem. Photobiol. A: Chem.* **1991**, *53*, 233–250.
(8) Hurter, P. N.; Hatton, T. A. *Langmuir* **1992**, *8*, 1291–1299.
(9) Leibler, L.; Orland, H.; Wheeler, J. C. *J. Chem. Phys.* **1983**, *79*, 3550–3557.
(10) Noolandi, J.; Hong, K. M. *Macromolecules* **1983**, *16*, 1443–1448.
(11) Munch, M. R.; Gast, A. P. *Macromolecules* **1988**, *21*, 1360–1366.
(12) Nagarajan, R.; Ganesh, K. *J. Chem. Phys.* **1989**, *90*, 5843–5856.
(13) Halperin, A. *Macromolecules* **1987**, *20*, 2943–2946.
(14) Marques, C. N. *Macromolecules* **1988**, *21*, 1051.
(15) Semenov, A. N. *Sov. Phys.—JETP (Engl. Transl.)* **1985**, *61*, 733.
(16) Zhulina, Y. B.; Birshtein, T. M. *Polym. Sci. USSR (Engl. Transl.)* **1986**, *12*, 2880–2886.
(17) van Lent, B.; Scheutjens, J. M. H. M. *Macromolecules* **1989**, *22*, 1931–1937.
(18) Wang, Y.; Mattice, W. L.; Napper, D. H. *Langmuir* **1993**, *9*, 66.
(19) Nagarajan, R.; Ganesh, K. *Macromolecules* **1989**, *22*, 4312–4325.
(20) Scheutjens, J. M. H. M.; Fleer, G. J. *J. Phys. Chem.* **1979**, *83*, 1619–1635.
(21) Evers, O. A.; Scheutjens, J. M. H. M.; Fleer, G. J. *Macromolecules* **1990**, *23*, 5221–5233.
(22) Scheutjens, J. M. H. M.; Fleer, G. J. *Macromolecules* **1985**, *18*, 1882–1900.
(23) Leermakers, F. A. M.; van der Schoot, P. P. A. M.; Scheutjens, J. M. H. M.; Lyklema, J. In *Surfactants in Solution*; Mittal, K. L., Ed.; Plenum Publishing Corp.: New York, 1989; Vol. 7, pp 43–60.

(24) Leermakers, F. A. M.; Scheutjens, J. M. H. M. *J. Phys. Chem.* **1989**, *93*, 7417–7426.
(25) Leermakers, F. A. M.; Scheutjens, J. M. H. M.; Lyklema, J. *Biophys. Chem.* **1983**, *18*, 353–360.
(26) Scheutjens, J. M. H. M.; Leermakers, F. A. M.; Besseling, N. A. M.; Lyklema, J. In *Surfactants in Solution*: Mittal, K. L., Ed.; Plenum Publishing Corp.: New York, 1989; Vol. 7, pp 25–42.
(27) Flory, P. J. *Principles of Polymer Chemistry*; Cornell University Press: Ithaca, NY, 1953.
(28) Hall, D. G. In *Nonionic Surfactants*; Schick, M. J., Ed.; Marcel Dekker: New York, 1987; Vol. 23, pp 233–296.
(29) Hill, T. L. *Thermodynamics of Small Systems*; Benjamin: New York, 1963; Vol. 1.
(30) Hill, T. L. *Thermodynamics of Small Systems*; Benjamin: New York, 1964; Vol. 2.
(31) Hall, D. G.; Pethica, B. A. In *Nonionic Surfactants*; Schick, M. J., Ed.; Marcel Dekker: New York, 1967.
(32) Hurter, P. N.; Scheutjens, J. M. H. M.; Hatton, T. A. *Macromolecules* **1993**, *26*, 5030.
(33) May, W. E.; Wasik, S. P.; Freeman, D. H. *Anal. Chem.* **1978**, *50*, 175–179.
(34) Malcolm, G. N.; Rowlinson, J. S. *Trans. Faraday Soc.* **1957**, *53*, 921–931.
(35) May, W. E.; Wasik, S. P.; Freeman, D. H. *Anal. Chem.* **1978**, *50*, 997–1000.
(36) Booth, C.; Devoy, C. J. *Polymer* **1971**, *12*, 309.
(37) Bailey, A. I.; Saleme, B. K.; Walsh, D. J.; Zeytountsian, A. *Colloid Polym. Sci.* **1979**, *257*, 948–952.
(38) Helfand, E.; Tagami, Y. *Polym. Lett.* **1971**, *9*, 741–746.